

Solution of the kinetic equation for the deposited-momentum distribution: neglecting threshold energy (atomic impact)

This article has been downloaded from IOPscience. Please scroll down to see the full text article.

1994 J. Phys.: Condens. Matter 6 10647

(<http://iopscience.iop.org/0953-8984/6/49/008>)

View [the table of contents for this issue](#), or go to the [journal homepage](#) for more

Download details:

IP Address: 171.66.16.179

The article was downloaded on 13/05/2010 at 11:28

Please note that [terms and conditions apply](#).

Solution of the kinetic equation for the deposited-momentum distribution: neglecting threshold energy

L G Glazov

High Current Electronics Institute, Akademichesky, 4, Tomsk, Russia

Received 15 April 1994, in final form 18 August 1994

Abstract. A regular method for finding solutions of the equation for the depth distribution of momentum deposited by atomic particles in elastic collisions is developed, using the model of an infinite medium and power cross section. It is shown that in neglecting threshold energy the distribution has a specific singularity at the target surface; its physical origin and the respective asymptotes are investigated. The calculated distributions and other functions connected with the problem are given.

1. Introduction

The present paper is devoted to a new investigation of the known problem of finding the deposited-momentum depth distributions for interaction between ions and amorphous or polycrystalline targets in the linear cascade model [1, 2, 3]. This function is of primary interest for damage cascade theory, especially because of the well-known applications to sputtering and recoil implantation [1, 2, 3, 4].

The following circumstances require a new analysis of this problem. The theoretical description of momentum deposition is based on integro-differential equations of the same kind as for the deposited-energy distribution, and leads to the problem of reconstructing a function to be found from its spatial moments. It has been pointed out [2] that this problem appears to be more difficult for momentum deposition, because the corresponding profile is not a positive-definite function, and traditional methods do not demonstrate appropriate convergence. Definite progress was achieved by using the Padé approximants method [5], which seemed to give reasonable results [2]; but critical analysis of these results shows that some important features of the solution were not clear in this approach either.

First, it can be readily shown immediately from the kinetic equation for the deposited-momentum depth profile that if we neglect threshold energy [6] this function has a specific singularity at the target surface. This is an important qualitative feature of the deposited-momentum distribution and cannot be ignored when building the profile to be found from the spatial moments; moreover, the correct description of the behaviour of the function in the target surface region is especially necessary because of the sputtering theory applications.

Second, we are going to show, furthermore, that threshold energy effects (which are usually assumed to be reasonably negligible in semi-analytical investigations) need to be taken into account for correct calculation of some important functions of the problem—in particular, for finding the value of the distribution at the target surface. From the

mathematical point of view, this situation arises because in general the threshold energy correction to the distribution is *not* of the same order as the one to the spatial moments, and in some cases appears to be governing or comparable with the respective values in the $W = 0$ model. On the other hand, on introducing threshold energy into the kinetic equation one can obtain interesting analytical and numerical results in this direction.

The solution of the kinetic equation taking into account the factors itemized above can be obtained by using a modification of the regular method developed in [7] for finding the deposited-energy profiles. This method is based upon calculating the spatial moments with high accuracy, immediate tabulation of the Taylor series for the Fourier transform of the distribution and the subsequent continuation of the latter in accordance with analytically established asymptotic expressions.

Let us adopt a relatively simple model of the phenomenon: an infinite isotropic random medium, neglect of electronic energy losses, and a power cross section of elastic collisions. For simplicity, we discuss only the case of equal masses of an ion and a target atom.

The evaluation in the present paper is given only for the component of momentum normal to the target surface ($P_x(x, E, \theta)$ in the notation of [2]); it is the most interesting function, because it is not positive-definite and it is assumed to determine anisotropic corrections to the sputtering yield [1, 3, 8] in the sputtering theory. Correspondingly results for other components can be obtained by the same method.

In the present paper we are going to discuss only solutions neglecting threshold energy. In this model, the deposited-momentum distribution reduces to the momentum per unit depth of cascade particles after the energy dissipation has proceeded to essentially the zero-energy level, determined as an average over many slowing-down events. The evaluation in the $W \neq 0$ case requires a knowledge of the $W = 0$ results and requires a specific mathematical technique. The $W \neq 0$ corrections will be considered in a future paper.

2. Equations governing momentum deposition

If we neglect threshold energy and electronic stopping, the kinetic equation for the deposited-momentum depth distribution $P(z, E, e)$ in an infinite medium is [2]:

$$-\eta \frac{\partial}{\partial z} P(z, E, e) = N \int d\sigma [P(z, E, e) - P(z, E - T, e') - P(z, T, e'')] \quad (1)$$

where $P(z, E, e) dz$ is an average momentum deposited in the interval $(z, z + dz)$ during the development of the cascade caused by one projectile, z is the coordinate along the inner normal to the target surface, and $z = 0$ at the surface; E is the initial energy of a projectile; e, e', e'' are the unit vectors in the directions of the starting, scattered and recoiling particle velocities respectively; T is the energy transfer in an elastic collision; $d\sigma$ is the corresponding differential cross section; η is the direction cosine of e with respect to the z -axis; and N is the density of the target atoms.

From momentum conservation, we have also the normalization condition

$$\int_{-\infty}^{\infty} P(z, E, e) dz = Mv \quad (2)$$

where Mv is the initial momentum of the projectile.

In the case of the power cross section [9, 6, 3]

$$d\sigma(E, T) = CE^{-m}T^{-1-m} dT \quad 0 < m < 1 \quad (3)$$

the function to be found satisfies a simple scaling law, and can be represented in the form:

$$P_z(z, E, e) = \frac{1}{3}(2M)^{1/2}NCE^{1/2-2m}F(x, \eta) \tag{4}$$

where $x = zNC/E^{2m}$ and F is a dimensionless function. Expanding F in terms of Legendre polynomials

$$F(x, \eta) = \sum_{l=0}^{\infty} (2l+1)P_l(\eta)F_l(x) \tag{5}$$

one can obtain by the usual method [6] the system of integro-differential equations for the functions $F_l(x)$ ($F_{-1} \equiv 0$):

$$\begin{aligned} -\frac{d}{dx}[lF_{l-1}(x) + (l+1)F_{l+1}(x)] \\ = (2l+1) \int_0^1 t^{-1-m} dt \left\{ F_l(x) - P_l(\sqrt{1-t})(1-t)^{1/2-2m} F_l(x/(1-t)^{2m}) \right. \\ \left. - P_l(\sqrt{t})t^{1/2-2m} F_l(x/t^{2m}) \right\} \end{aligned} \tag{6}$$

and the normalization conditions:

$$\int_{-\infty}^{\infty} F_l(x) dx = \delta_{l1}. \tag{7}$$

The functions F_l with odd and even l are symmetric and antisymmetric respectively.

Introducing the spatial moments

$$\left\{ \begin{matrix} F_l^n(\eta) \\ F_l^n \end{matrix} \right\} = \int_{-\infty}^{\infty} x^n \left\{ \begin{matrix} F(x, \eta) \\ F_l(x) \end{matrix} \right\} dx \tag{8}$$

one can easily obtain from equations (6) the following recurrence relations:

$$F_l^n = \frac{n[lF_{l-1}^{n-1} + (l+1)F_{l+1}^{n-1}]}{(2l+1)I_l(2mn+1/2)} \tag{9}$$

where

$$I_l(s) = \int_0^1 t^{-1-m} dt \left[1 - P_l(\sqrt{1-t})(1-t)^s - P_l(\sqrt{t})t^s \right]$$

and can be expressed in terms of the beta function [6, 7]. The formulae (9) make it possible to calculate the moments of the distribution to be found with arbitrary necessary accuracy, using the normalization conditions (7) as starting values for the recurrence procedure.

Let us introduce also the Fourier transforms $f(k, \eta)$, $f_l(k)$:

$$\left\{ \begin{matrix} F(x, \eta) \\ F_l(x) \end{matrix} \right\} = \frac{1}{2\pi} \int_{-\infty}^{\infty} e^{ikx} \left\{ \begin{matrix} f(k, \eta) \\ f_l(k) \end{matrix} \right\} dk.$$

The functions $f_l(k)$ satisfy to the system of equations

$$\begin{aligned} -ik[lf_{l-1}(k) + (l+1)f_{l+1}(k)] \\ = (2l+1) \int_0^1 t^{-1-m} dt \left[f_l(k) - P_l(\sqrt{1-t})(1-t)^{1/2} f_l(k(1-t)^{2m}) \right. \\ \left. - P_l(\sqrt{t})t^{1/2} f_l(kt^{2m}) \right] \end{aligned} \tag{10}$$

which can be readily derived from (6). The functions f_{2l+1} are real and symmetric functions of k , while the f_{2l} are imaginary and antisymmetric.

Knowing F^n one can tabulate the Fourier transform of the deposited-momentum distribution in accordance with the Taylor expansion of the latter:

$$f(k, \eta) = \sum_{n=0}^{\infty} (-ik)^n F^n(\eta)/n! \quad (11)$$

Analogous formulae arise for the functions $f_l(k)$.

3. The asymptotic behaviour of the functions for the cases $k \rightarrow \infty$ and $x \rightarrow 0$

By calculating the moments and tabulating the series (11), one can obtain $f(k, \eta)$ up to some value $k = k_0$ depending on the adopted accuracy of calculating the moments. Then one has to make the correct continuation of the Fourier transform in the region $k > k_0$. The function $f(k, \eta)$ very slowly decreases when $k \rightarrow \infty$, because $F(x, \eta)$ at least is not differentiable at $x = 0$. The latter can be verified directly from the equations (6). Hence it is necessary to investigate the asymptotes of the functions at $k \rightarrow \infty$ and $x \rightarrow 0$ for the correct continuation of the Fourier transform in the region $k > k_0$ and an understanding of the characteristic features of the behaviour of $F(x, \eta)$ near the target surface.

3.1. The $x \rightarrow 0$ asymptotes

When $x \rightarrow 0$, the last term on the right-hand side of (6) appears to be the leading one. Let us examine the case $l = 0$, $x \rightarrow +0$:

$$\frac{dF_1(x)}{dx} \sim \int_0^1 t^{-1/2-3m} F_0(x/t^{2m}) dt = \frac{1}{2m} x^{-3/2+1/(4m)} \int_x^\infty \xi^{1/2-1/(4m)} F_0(\xi) d\xi.$$

Let us assume that $F_0(x)$ is finite near the point $x = 0$. Then the last integral appears finite when $x \rightarrow +0$ at least for $m > 1/6$, and the leading term of the asymptote reads as follows:

$$\frac{dF_1(x)}{dx} \sim \text{constant} \times x^{-3/2+1/(4m)}$$

and, consequently,

$$F_1(x) \sim \begin{cases} \text{constant} + \text{constant} \times x^{-1/2+1/(4m)} + \dots & m \neq 1/2 \\ \text{constant} \times \ln x + \text{constant} + \dots & m = 1/2 \end{cases} \quad (12)$$

and symmetrically for $x \rightarrow -0$. Thus, the derivative of $F_1(x)$ appears infinite when $x \rightarrow \pm 0$, and the function $F_1(x)$ itself has the logarithmic and power singularity at $x = 0$ for $m = 1/2$ and $m > 1/2$ respectively. The presence of the singularity can also be demonstrated directly from equation (6) by integrating over x from 0 to ∞ . Thus gives

$$F_1(0) = \int_0^\infty F_0(x) dx \int_0^1 t^{-1-m} dt \{1 - (1-t)^{1/2} - t^{1/2}\}.$$

The last integral diverges for $m \geq 1/2$.

In the case $l = 1$, $x \rightarrow +0$ we obtain from (6):

$$\frac{d}{dx}[F_0(x) + 2F_2(x)] \sim 3 \int_0^1 t^{-3m} dt F_1(x/t^{2m}) = \frac{3}{2m} x^{1/(2m)-3/2} \int_x^\infty \xi^{1/2-1/(2m)} F_1(\xi) d\xi.$$

The functions F_l with even l are antisymmetric, $F_{2l}(0) = 0$, so the leading terms of the asymptotic expansion are as follows:

$$F_0(x) + 2F_2(x) \sim \begin{cases} \text{constant} \times x^{1/(2m)-1/2} + \dots & m > 1/3 \\ \text{constant} \times x \ln x + \text{constant} \times x + \dots & m = 1/3 \end{cases} \quad (13)$$

and antisymmetrically for $x \rightarrow -0$.

The formulae (12), (13) can easily be extended to all functions with odd and even l respectively. Thus, the symmetric functions F_{2l+1} have the above specified singularity at the target surface; for $m \geq 1/3$ the antisymmetric functions F_{2l} have infinite derivatives at $x = 0$.

3.2. The $k \rightarrow \infty$ asymptotes and the method of numerical evaluation

The $k \rightarrow \infty$ asymptotes can be found from (10) in a similar way (see also the analogous evaluation in [7]). The corresponding results are as follows:

$$f_l(k) \sim \begin{cases} \text{constant} \times |k|^{-\frac{1}{2m}} & \text{odd } l, k \rightarrow \pm\infty \\ \text{sgn}(k)[\text{constant} \times |k|^{-\frac{1}{2}-\frac{1}{2m}} + \text{constant} \times |k|^{-\frac{3}{2}-\frac{1}{4m}}] & \text{even } l, k \rightarrow \pm\infty. \end{cases} \quad (14)$$

The function $f(k, \eta)$ can be divided into real and imaginary parts:

$$f(k, \eta) = f_S(k, \eta) + i f_A(k, \eta)$$

$$f_S(k, \eta) = f_S(-k, \eta) = -f_S(k, -\eta) \quad f_A(k, \eta) = -f_A(-k, \eta) = f_A(k, -\eta).$$

The functions f_S and f_A determine the symmetric and antisymmetric (on x) parts of $F(x, \eta)$:

$$F(x, \eta) = F_S(x, \eta) + F_A(x, \eta) \quad (15)$$

$$\begin{Bmatrix} F_S(x, \eta) \\ F_A(x, \eta) \end{Bmatrix} = \pm \frac{1}{\pi} \int_0^\infty \begin{Bmatrix} \cos(kx) f_S(k, \eta) \\ \sin(kx) f_A(k, \eta) \end{Bmatrix} dk. \quad (16)$$

The functions F_S, f_S and F_A, f_A include the terms with odd and even l respectively in the Legendre polynomials expansion, and their $x \rightarrow 0$ and $k \rightarrow \infty$ asymptotes are determined by formulae like (12), (13), (14).

The following procedure was used for numerically tabulating the solutions of the kinetic equation in the present paper. The moments of the distribution were calculated according to the recurrence formulae (9) with high accuracy (usually the moments were found up to $n = 300$ with 28-decimal-digits precision) to reach as high values of k as is possible by directly summing the series (11). Then the function $f(k, \eta)$ was tabulated using the formula (11) up to some value $k = k_0$, where the series can be calculated with sufficient accuracy (usually k_0 was taken to be equal to 30 for $m = 1/2$ and 12 for $m = 1/3$). Further, the Fourier transform was continued in the region $k > k_0$ separately for the real and imaginary parts of $f(k, \eta)$ by determining constants in the asymptotic formulae from the condition of best coincidence near the point $k = k_0$; the final result was obtained via the formulae (15), (16). The same method can also be used for tabulating the functions F_l if necessary.

4. Results and discussion

Figures 1(a) and 1(b) demonstrate the characteristic behaviour of the Fourier transforms $\text{Re } f$ and $\text{Im } f$. The Fourier transforms are shown up to $k = k_0$ used for the tabulation. In accordance with the asymptotic expressions given above, the functions are characterized by very slow decrease for large k .

The zeroth and first angular harmonics of the distribution for $m = 1/2$ are shown in figure 2. The function F_1 has a logarithmic singularity at $x = 0$; the derivative of F_0 is infinite at the target surface.

Analogous behaviour is demonstrated by the symmetric and antisymmetric parts of the function, which are shown in figures 3(a) and 3(b) for $\eta = 1$. For large enough negative x

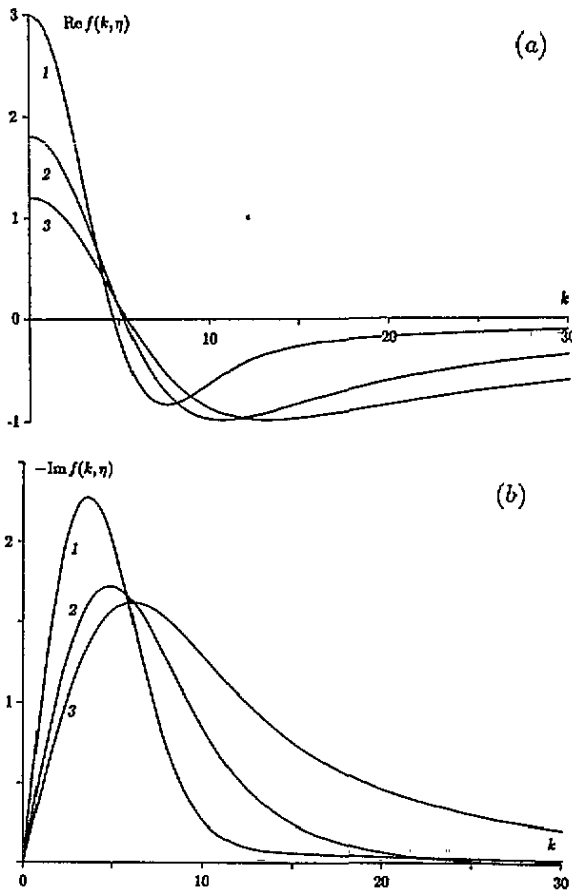


Figure 1. Dependencies of the real (a) and imaginary (b) parts of the Fourier transform $f(k, \eta)$ on k ; $m = 1/2$; $\eta = 1$ (1), $\eta = 0.6$ (2), $\eta = 0.4$ (3).

they compensate each other with good precision, providing small values of $F(x, \eta)$. Taking into account the independence of finding asymptotes for their Fourier transforms, this is an additional confirmation of the good accuracy of the results obtained.

Figure 4 demonstrates the functions $F(x, \eta)$ for normal and tangential incidence of an ion for $m = 1/2$. The model of an infinite medium is not appropriate for $\eta = 0$; however, the results are of definite interest from the mathematical point of view, because in this case F_S disappears and the solution is characterized by a behaviour that is typical for antisymmetric functions of the problem. Furthermore, $F(x, \eta = 0)$ can be considered as the deposited-momentum distribution in the perpendicular direction for normal incidence.

Figures 5(a) and (b) show the profiles $F(x, \eta)$ for different values of η . According to the general asymptotic features discussed above, the distributions for $m = 1/2$ have a logarithmic singularity at the target surface; the solutions for $m = 1/3$ have an infinite derivative at $x = \pm 0$, which changes sign at the surface.

Let us discuss the particular behaviour of the deposited-momentum distribution $P_z(z, E, e)$ and its physical origin.

The function $P_z(z, E, e)$ is not positive-definite. Momentum deposited inside the target ($z > 0$) must point in the positive z -direction at large penetration depths. Analogously, the

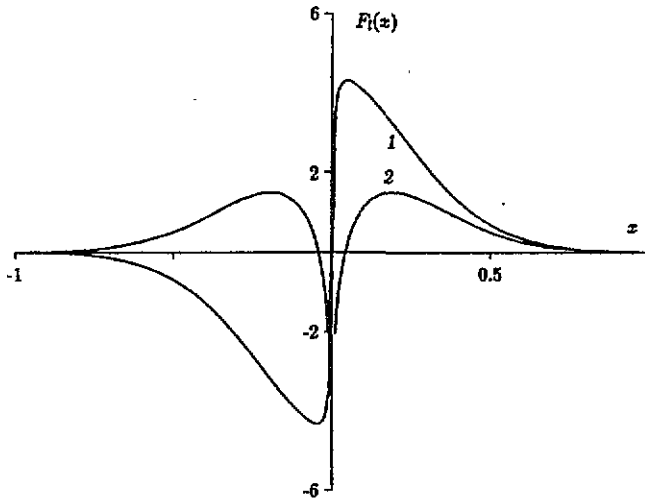


Figure 2. Dependencies $F_l(x)$ for $m = 1/2$; $l = 0(1)$ and $l = 1(2)$.

recoils, which reach large depths outside the target ($z < 0$), have predominantly negative z -components of momenta and provide negative values of the distribution. The last statement is definitely confirmed by the present calculations, in contrast with results from the formal Padé approximants method [2].

For direction cosines of a projectile, that are not too small the deposited-momentum distribution readily reaches a minimum at $z = 0$ and has relatively high negative values near the target surface. The presence of the minimum near $z = 0$ was indicated also by the earlier calculations [2], which nevertheless did not demonstrate the following particular features:

- (i) the minimum is located exactly at the target surface, since the spatial derivative abruptly changes sign at $z = 0$;
- (ii) the function is not smooth at the target surface, its derivative appears to be infinite at $z = \pm 0$;
- (iii) the function itself is infinite at $z = 0$ for $m \geq 1/2$.

These characteristic features were established above in the formal mathematical manner. Now we are going to consider the physical origin of the rapidly reached minimum at the target surface and the qualitative features itemized above.

From the physical point of view, the rapidly reached minimum of the distribution is created by contributions of the sub-cascades initiated by atoms, which are caused to recoil by the projectile in the target surface region, the effect being determined mainly by relatively low-energy recoils. In fact, we show below that the primary recoils, starting, say, from $z = z_0$, lead to comparatively very large negative and positive contributions to the distribution in some narrow regions on the left and on the right of $z = z_0$ respectively. The positive contribution at $z > z_0$ appears to be effectively compensated by the negative parts of the contributions of sub-cascades caused by atoms, which are caused to recoil by a projectile at larger penetration depths, but the negative contributions of sub-cascades caused by primary recoils starting from some narrow target surface region have no compensation and create the rapidly reached minimum at $z = 0$.

Let us consider a more quantitative estimation of this effect for the special case of

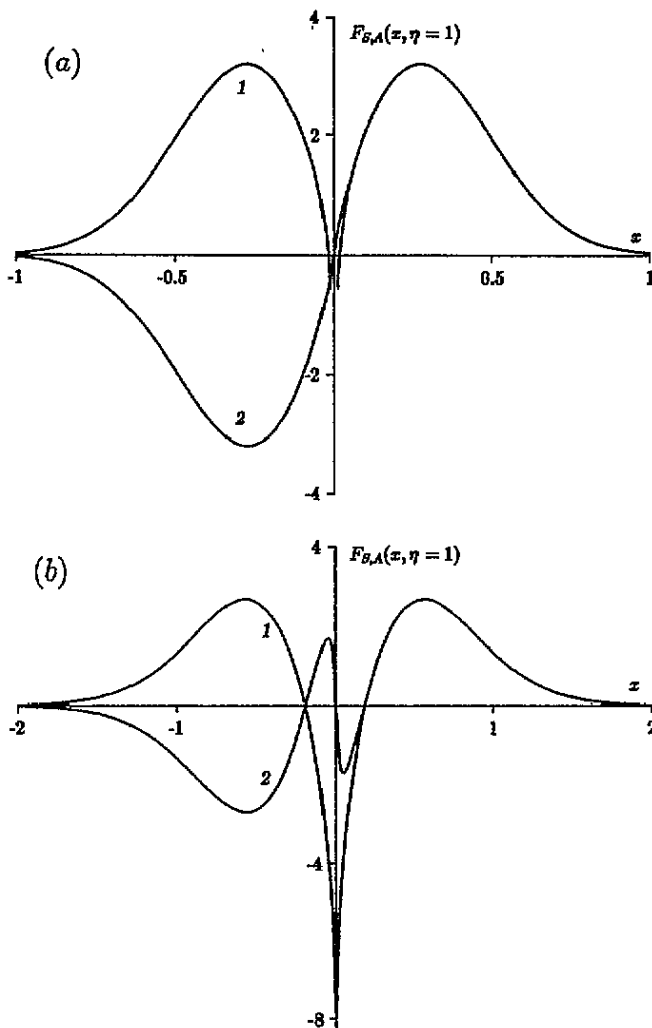


Figure 3. Symmetric (1) and antisymmetric (2) parts of $F(x, \eta = 1)$; $m = 1/2$ (a) and $m = 1/3$ (b).

normal incidence of a projectile ($\eta = 1$). First, we introduce the quantity

$$\sigma_A(E) = \int_0^E (T/E)^{1/2} d\sigma(E, T)$$

where the transferred energy T is the recoil energy. The central role of $\sigma_A(E)$ in estimations of this kind is shown by the following: $Np(E)\sigma_A(E) \delta z$ is the average sum of absolute values of momentums of recoils created by a projectile of mass M , energy E and momentum $p(E) = (2ME)^{1/2}$ in travelling a distance δz . For the power cross-section (3) and cross-sections with similar $T/E \ll 1$ asymptotes, the quantity $\sigma_A(E)$ is significantly larger than, say, the momentum transfer cross-section

$$\sigma_{tr}(E) = \int [1 - (e \cdot e')(1 - T/E)^{1/2}] d\sigma = \int_0^E (T/E) d\sigma(E, T)$$

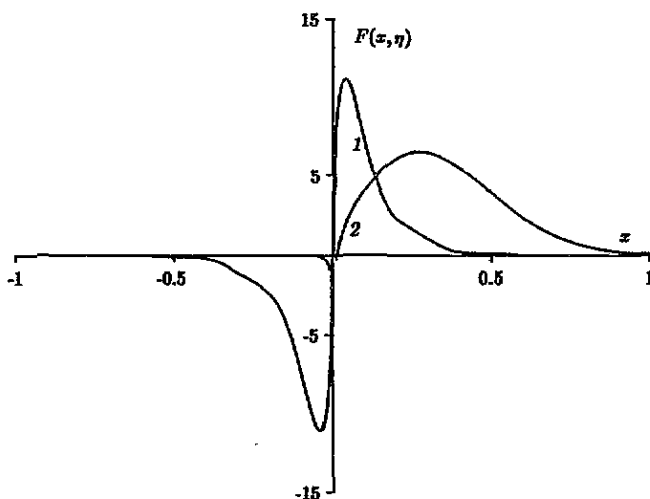


Figure 4. Dependencies $F(x, \eta)$ for tangential and normal incidence; $m = 1/2$; $\eta = 0$ (1), $\eta = 1$ (2).

which is dominated by the contribution of relatively low-energy recoils, whose velocities are approximately perpendicular to the direction of motion of a projectile.

To estimate the effect of sub-cascades initiated by primary recoils created in the target surface region, we adopt for a moment the following simple model:

(i) we neglect energy losses and the scattering of a projectile;

(ii) taking into account the leading role of low-energy primary recoils, we assume that the primary recoils start perpendicularly to the direction of motion of a projectile, i.e., in the $\eta = 1$ case, their direction cosine $\eta'' = 0$.

Then, any recoil of energy T starting from a point $z = z_0$ provides on average the contribution $P_z(z - z_0, T, \eta = 0)$ into the distribution. For $m = 1/2$, the function $P_z(z, E, \eta = 0)$ in dimensionless units is shown in figure 4. In general, the antisymmetric function $P_z(z, E, \eta = 0)$ is predominantly negative and positive for $z < 0$ and $z > 0$ respectively. The maximum and the minimum of $P_z(z, E, \eta = 0)$ are located at $|z| = \alpha E^{2m}/NC$, and the integrals

$$\int_0^{\infty} P_z(z, E, \eta = 0) dz = - \int_{-\infty}^0 P_z(z, E, \eta = 0) dz = \beta p(E)$$

where the coefficients $\alpha \lesssim 1/10$ and $\beta \sim 1/3$ depend relatively slightly on m . Here, for simplicity, we use a simple approximation for $P_z(z, E, \eta = 0)$:

$$P_z(z, E, \eta = 0) = \gamma(E) \operatorname{sgn}(z) \theta \left(\frac{2\alpha E^{2m}}{NC} - |z| \right)$$

where $\theta(x) = 1$ for $x \geq 0$ and $\theta(x) = 0$ for $x < 0$, $\gamma(E) = \beta NC p(E)/2\alpha E^{2m}$ being chosen to conserve correct values of the integrals

$$\int_0^{\pm\infty} P_z(z, E, \eta = 0) dz.$$

Using more realistic approximations for $P_z(z, E, \eta = 0)$, we would obtain qualitatively the same results, with slight corrections in coefficients in the final expressions for the $z \rightarrow 0$ asymptotes.

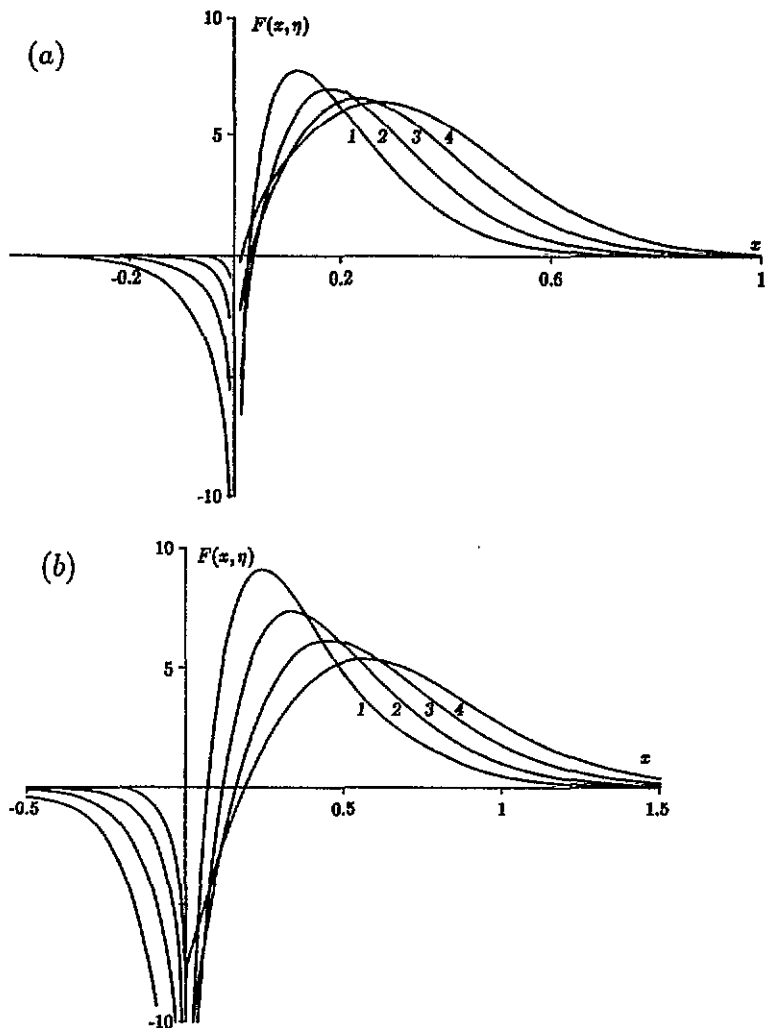


Figure 5. Dependencies $F(x, \eta)$ on x for $m = 1/2$ (a) and $m = 1/3$ (b); $\eta = 0.4$ (1), $\eta = 0.6$ (2), $\eta = 0.8$ (3), $\eta = 1$ (4).

In the adopted model, in travelling a distance $(z_0, z_0 + dz_0)$ a projectile creates on average

$$N dz_0 \frac{d\sigma(E, T)}{dT} dT$$

primary recoils of energy $(T, T + dT)$. They initiate sub-cascades which give a contribution

$$N dz_0 \frac{d\sigma(E, T)}{dT} dT P_z(z - z_0, T, \eta = 0)$$

into the deposited momentum-distribution. The positive part (at $z > z_0$) of this contribution is compensated by the negative part of the respective contribution of recoils created in the interval $(z_0 + 2\alpha T^{2m}/NC, z_0 + 2\alpha T^{2m}/NC + dz_0)$. So, integrating over z_0 and the recoil energy T , we find the following estimate for the deposited-momentum distribution near the

target surface:

$$\begin{aligned}
 P_z(z, E, \eta = 1) &\approx -N \int_0^E dT \frac{d\sigma(E, T)}{dT} \gamma(T) \\
 &\times \int_0^{2\alpha T^{2m}/NC} dz_0 \theta(z_0 - z) \theta\left(\frac{2\alpha T^{2m}}{NC} + z - z_0\right) \\
 &= -N \int_0^E dT \frac{d\sigma(E, T)}{dT} \gamma(T) \left[\frac{2\alpha T^{2m}}{NC} - |z|\right] \theta\left(\frac{2\alpha T^{2m}}{NC} - |z|\right).
 \end{aligned}$$

This integral can easily be calculated analytically and indicates the same leading $z \rightarrow 0$ asymptotic terms for the symmetric part of the distribution as in section 3; all qualitative features itemized above are demonstrated also; and using appropriate values of α and β , one finds estimates for the effective width and other characteristics of the rapidly reached minimum at $z = 0$, that appear to be in a reasonable agreement with the numerical tabulation results.

We consider in more detail the corresponding estimation for the deposited-momentum distribution at $z = 0$:

$$P_z(z, E, \eta = 1) \approx -N \int_0^E \frac{d\sigma(E, T)}{dT} \gamma(T) \frac{2\alpha T^{2m}}{NC} dT = -\beta N p(E) \sigma_A(E).$$

Thus, $|P_z(z, E, \eta = 1)|$ is approximately equal, apart from a trivial factor, to the average sum of absolute values of momenta of recoils created by a projectile per unit path length. The larger m , the greater the ratio $\sigma_A(E)/\sigma_H(E)$, because of the increasing contribution of low-energy primary recoils, and this provides a rapid growth of the relative altitude of the minimum at $z = 0$. The quantity $\sigma_A(E)$ becomes infinite for $m \geq 1/2$, leading to an infinite value of the distribution at the target surface, in agreement with the results of section 3.

An analogous evaluation can be done as well for $\eta \neq 1$, although it is more complicated because an additional integration over direction cosines of primary recoils appears to be necessary. The physical origin of the rapidly reached minimum at the target surface is qualitatively the same, apart from an angular dependence: primary recoils created at $z = z_0$ initiate sub-cascades, which give large (approximately proportional to the summized absolute values of recoils momenta) positive and negative contributions to $P_z(z, E, e)$ in narrow regions on the right and on the left of $z = z_0$ respectively; the absence of an effective compensation of the negative parts of these contributions for recoils created at small penetration depths produces the rapidly reached minimum at the target surface. The effect mainly arises because the average absolute value of primary recoil momentum is significantly larger than the corresponding component in the direction of motion of a projectile, due to the rapidity with which the maximum of the power cross-section (3) is approached as $T/E \rightarrow 0$. So, qualitatively the same particular behaviour of the distribution as is found near the target surface is also found for more complicated cross-sections, if their $T/E \ll 1$ asymptotes are similar to those given by (3).

It is necessary to make some comments on the threshold energy effects here. The simplest way to take these effects into account is introducing the boundary condition [6]

$$P(z, E, e) = Mv \delta(z) \quad E \leq W$$

with corresponding changes in the kinetic equation. Appropriate corrections to the spatial moments can be found by using the Robinson Laplace transformation method [10] and for $m > 1/4$ these are $\sim (W/E)^{2m-1/2}$. The larger m , the smaller these corrections; but the corresponding corrections to the values of the distribution in the target surface region (and,

in particular, to $P(z = 0, E, e)$, which is important for the theory of sputtering) change in an opposite way, such that for $m \geq 1/2$ no finite result for this region can be obtained while neglecting threshold energy. Of course, these corrections can hardly be neglected for slightly smaller values of m . The analytical and numerical evaluation for the latter case is now in progress and will be presented in a future paper.

References

- [1] Littmark U 1974 *Thesis* Copenhagen University
- [2] Littmark U and Sigmund P 1975 *J. Phys. D: Appl. Phys.* **8** 241
- [3] Sigmund P 1977 *Inelastic Ion-Surface Collisions* ed N H Tolk *et al* (New York: Academic) p 121
- [4] Falcone D 1990 *Rev. Nuovo Cimento* **13** 1
- [5] Chisholm J S R and Common A K 1970 *The Padé Approximant in Theoretical Physics* ed G A Baker and J L Gammel (New York: Academic) pp 183–95
- [6] Winterbon K B, Sigmund P and Sanders J B 1970 *Mat. Fys. Meddr. Dansk. Vidensk. Selsk.* **37** No 14
- [7] Glazov L G 1994 *J. Phys.: Condens. Matter* **6** 4181
- [8] Sigmund P 1969 *Phys. Rev.* **184** 383
- [9] Lindhard J, Nielsen V and Scharff M 1968 *Mat. Fys. Meddr. Dansk. Vidensk. Selsk.* **36** No 10
- [10] Robinson M T 1965 *Phil. Mag.* **12** 145